Neutrophil adhesion and chemotaxis depend on substrate mechanics

2010 J. Phys.: Condens. Matter 22 194117

(http://iopscience.iop.org/0953-8984/22/19/194117)

IOP Publishing Journal of Physics: Condensed Matter

J. Phys.: Condens. Matter **22** (2010) 194117 (14pp) doi:10.1088/0953-8984/22/19/194117

Neutrophil adhesion and chemotaxis depend on substrate mechanics

Risat A Jannat[1], Gregory P Robbins[2], Brendon G Ricart[2], Micah Dembo[3] and Daniel A Hammer[1,2,4]

[1] Department of Bioengineering, University of Pennsylvania, 240 Skirkanich Hall, 210 South 33rd Street, Philadelphia, PA 19104, USA
[2] Department of Chemical and Biomolecular Engineering, University of Pennsylvania, 311A Towne Building, 220 South 33rd Street, Philadelphia, PA 19104, USA
[3] Department of Biomedical Engineering, Boston University, 44 Cummington Street, Boston, MA 02215, USA

E-mail: hammer@seas.upenn.edu

Received 18 August 2009, in final form 30 December 2009
Published 26 April 2010
Online at stacks.iop.org/JPhysCM/22/194117

Abstract

Neutrophil adhesion to the vasculature and chemotaxis within tissues play critical roles in the inflammatory response to injury and pathogens. Unregulated neutrophil activity has been implicated in the progression of numerous chronic and acute diseases such as rheumatoid arthritis, asthma and sepsis. Cell migration of anchorage-dependent cells is known to depend on both chemical and mechanical interactions. Although neutrophil responses to chemical cues have been well characterized, little is known about the effect of underlying tissue mechanics on neutrophil adhesion and migration. To address this question, we quantified neutrophil migration and traction stresses on compliant hydrogel substrates with varying elasticity in a micromachined gradient chamber in which we could apply either a uniform concentration or a precise gradient of the bacterial chemoattractant fMLP. Neutrophils spread more extensively on substrates of greater stiffness. In addition, increasing the stiffness of the substrate leads to a significant increase in the chemotactic index for each fMLP gradient tested. As the substrate becomes stiffer, neutrophils generate higher traction forces without significant changes in cell speed. These forces are often displayed in pairs and focused in the uropod. Increases in the mean fMLP concentration beyond the K_D of the receptor lead to a decrease in chemotactic index on all surfaces. Blocking with an antibody against β_2-integrins leads to a significant reduction, but not an elimination, of directed motility on stiff materials, but no change in motility on soft materials, suggesting neutrophils can display both integrin-dependent and integrin-independent motility. These findings are critical for understanding how neutrophil migration may change in different mechanical environments *in vivo* and can be used to guide the design of migration inhibitors that more efficiently target inflammation.

(Some figures in this article are in colour only in the electronic version)

1. Introduction

Neutrophils are subject to numerous spatial and temporal cues in their normal physiological environment, including gradients of signaling molecules, mechanical interactions with surrounding tissues, and direct contacts with other cells (Simon and Green 2005). It is well appreciated that chemical cues exchanged between neutrophils and their environment play an important role in determining effector functions required for homeostasis and many detailed studies of such interactions have been reported (Tranquillo *et al* 1988, Devreotes and Zigmond 1988, Herzmark *et al* 2007). Unstimulated neutrophils are typically non-adherent, but their

[4] Address for correspondence: Department of Bioengineering, University of Pennsylvania, 240 Skirkanich Hall, 210 S. 33rd Street, Philadelphia, PA 19104, USA.

adhesiveness can be upregulated by chemoattractants within minutes (Alon and Ley 2008).

Sequential interactions between neutrophil receptors and endothelium-bound adhesion ligands such as selectins and ICAMs lead to rolling, firm adhesion, migration and transmigration. β_2 integrin receptors such as LFA-1 and Mac-1, are the most relevant for neutrophil adhesion and migration. Active conformations of integrins on a neutrophil can be induced by chemoattractant binding to G-protein coupled receptors through inside-out signaling or by direct ligand binding through outside-in signaling (Alon and Ley 2008). Mechanical forces loaded onto integrin receptors during outside-in signaling can accelerate conformational rearrangements leading to stabilization of high affinity conformations and cell arrest (Puklin-Faucher *et al* 2006). After migration along a blood vessel wall to an appropriate gap junction, a neutrophil transmigrates through the endothelium into the surrounding extracellular matrix. Neutrophils are capable of infiltrating virtually every organ within the body. Therefore, the ability of a neutrophil to navigate through diverse mechanical environments is critical to tissue homeostasis and host defense.

Previous studies of anchorage-dependent cell motility have elucidated how cells of endothelial, epithelial or fibroblast origin process mechanical information in their surroundings (Reinhart-King *et al* 2003, Paszek *et al* 2005, Reinhart-King *et al* 2005, 2008, Smith *et al* 2007, Dembo and Wang 1999, Beningo *et al* 2001, Munevar *et al* 2001a, 2001b, Balaban *et al* 2001). These studies have uncovered a number of important principles, namely that anchorage-dependent cells are capable of sensing and responding to changes in the biophysical properties of their underlying two-dimensional matrices through integrin receptors and focal adhesions (Dembo and Wang 1999, Choquet *et al* 1997, Reinhart-King *et al* 2005, Balaban *et al* 2001, Gupton and Waterman-Storer 2006). In order to migrate, anchorage-dependent cells must adhere to and generate tension on their underlying substrates through integrin receptors. In the towing model of cell motion, cells must extend their lamellipodia and grab hold of the substrate through integrins, generate cellular contraction which requires exerting tension on the substrate and then release the uropod which likely requires exertion of mechanical forces or weakened substrate adhesion, or both (Munevar *et al* 2001a, 2001b). Another key concept elucidated from prior studies of cell migration is the presence of a biphasic relationship between cell speed and substrate ligand density or substrate mechanics (Palecek *et al* 1997, Peyton and Putnam 2005). It has been shown that maximal migration speeds are typically observed at intermediate levels of adhesion where a balance between generation of propulsive forces within the lamellipod and retraction of the cell body at the rear is achieved.

Given that integrins are required to exert forces on a substrate, substrate compliance should modulate the local concentration of adhesive stresses under a cell; in turn, for a given applied force, substrate compliance could modulate the clustering of adhesion receptors and hence signaling. Pelham and Wang (1997) showed that the compliance of the substrate could affect the size of focal adhesions as well as the rate of cell migration. Specifically, they showed that 3T3 and NRK cells have higher rates of cell motility and lamellipodial ruffling, respectively, when substrate rigidity is decreased (Pelham and Wang 1997). Recently, Chen and Odde (2008) showed that molecular clutches involving actin and myosin link the cell to the substrate and act as a motor–clutch system that can inherently sense and respond to the elasticity of the substrate. A recent theoretical model from our laboratory (Paszek *et al* 2009) illustrates that substrate stiffness can induce receptor clustering by presenting an energy barrier preventing integrins from becoming dispersed. Consistent with the idea that substrate mechanics can alter cell motility, Lo and co-workers presented evidence of durotaxis, in which cells migrate toward stiffer regions of the substrate (Lo *et al* 2000).

A further question is how tensions and forces within compliant substrates affect adhesion and motility. Forces generated though the substrate can lead to biochemical responses through outside-in signaling, such as phosphorylation, as well as the recruitment of scaffold proteins; then, further downstream signaling pathways are activated leading to changes in cell morphology and motility (Giannone and Sheetz 2006). However, the role of tension in durotaxis is not well defined. There is conflicting evidence that tension controls receptor clustering. Beningo and co-workers indicated that tension preceded the formation of focal adhesions (Beningo *et al* 2001), but Balaban and co-workers presented contrary results that suggested tension is generated when or after focal adhesions form (Balaban *et al* 2001). The correlation between substrate tension and motility is still unclear and needs to be studied further.

Despite the importance of neutrophils and other amoeboid cells of the immune system, relatively little has been done to probe the mechanochemical control of neutrophil migration. Classic studies performed by Zigmond and co-workers on glass surfaces have demonstrated that neutrophil responses are influenced by both the mean chemoattractant concentration and the slope of the gradient of concentration (Devreotes and Zigmond 1988, Tranquillo *et al* 1988). Recently, we showed that the traction stresses of neutrophils, which migrate rapidly and do not form focal adhesions, could be measured by traction force microscopy (TFM) despite being relatively weak compared to fibroblasts and other endothelial cells (Smith *et al* 2007). TFM images showed that, during both chemokinesis and chemotaxis toward a chemoattractant exuded from a pipette, neutrophils display a contractile stress that is concentrated in the uropod which appears to drive motion through tail contraction (Smith *et al* 2007). Other amoeboid cells such as Dictyostelium also display maps of traction stresses with high concentrations of traction stresses in the uropod (Lombardi *et al* 2007), suggesting a shared mechanism of locomotion among amoeboid cells.

Since motility in neutrophils is associated with tail contraction, membrane interactions with a substrate, which are in turn affected by substrate compliance, might affect neutrophil motility. Recently, Oakes and co-workers showed that, on fibronectin-coated gels of different compliances, neutrophils spread and crawl best on stiffer gels and appear to

move more faithfully toward chemoattractants delivered from a pipette (Oakes *et al* 2009). Further, based on a different imaging methodology, they substantially confirmed the role of tail contraction in leukocytes by showing that traction stresses were mainly distributed between the uropod and the mid-section of the cells as motility progresses. In this paper, we will describe experiments conducted contemporaneously which both complement and extend this work at higher resolution (Jannat 2009).

In essence, our approach is to use a custom micromachined chamber to make precise gradients of the bacterial chemoattractant fMLP, and to measure the chemotactic response of neutrophils on gels of different elasticity coated with ICAM-1. On each gel we are thereby able to quantify the changes in neutrophil responses as a function of two important chemical cues, the mean concentration of chemoattractant and the steepness of an fMLP gradient. We find that the response of a neutrophil to these cues can vary significantly depending on the mechanical properties of the underlying substrate. To explore how this tactile response depends on integrin-mediated signaling pathways, we blocked integrin molecules and measured the effect on migration parameters. Our results show that integrin engagement is required for motility on stiff hydrogels (12 kPa), but not on soft hydrogels (2 kPa). Furthermore, high resolution TFM imaging of the traction stresses indicate that, during chemotaxis on stiffer gels, centers of force and contraction are punctate, well organized, and highly localized to the uropod. These force centers weaken during motility on softer gels. Thus, the mechanism of directed neutrophil chemotaxis is markedly different depending on the mechanical environment and includes a complex interplay of chemical signaling and interfacial mechanics.

2. Materials and methods

2.1. Reagents

Adhesive ligands were protein G (Pierce Biochemicals, Rockford, IL), human ICAM-1 Fc, and E-Selectin Fc (R&D Systems, Minneapolis, MN). TS1/18 $\beta 2$ integrin antibody was used at 10 μg ml^{-1} to block cell surface receptors (Pierce Biochemicals, Rockford, IL), Neutrophils were activated with fMLP chemoattractant peptide (Sigma-Aldrich, St Louis, MO), Cell contractility through RhoA was inhibited using 10 μM Y-26732 ROCK inhibitor (Calbiochem, San Diego, CA).

2.2. Isolation of neutrophils

Whole blood was obtained from healthy human donors by venipuncture and collected in BD Vacutainer tubes containing citrate-EDTA anticoagulant (Becton Dickinson, Franklin Lakes, NJ). Whole blood was layered onto Polymorphprep density gradient medium (Axis-Shield, Oslo, Norway) and centrifuged at 500 g for 1 h. After centrifugation, the neutrophil fraction was aspirated and washed once by centrifugation in HBSS without Ca^{2+} and Mg^{2+}. Washed neutrophils were then resuspended in HBSS without Ca^{2+} and Mg^{2+} supplemented with 0.1% human serum (Sigma-Aldrich, St Louis, MO) and 10 mM HEPES (Invitrogen, Carlsbad, CA). Prior to use in flow chamber assays, the neutrophil solution was supplemented with Ca^{2+} and Mg^{2+}.

2.3. Preparation of hydrogel substrates

Polyacrylamide hydrogels were prepared as described previously with slight modifications (Pelham and Wang 1997). Briefly, Corning rectangular glass coverslips were passed through the flame of a Bunsen burner, swabbed with 0.1 N NaOH solution and allowed to air-dry. Coverslips were coated with 3-aminopropyl-trimethoxysilane (APTS, Sigma-Aldrich, St Louis, MO) and allowed to dry for several minutes inside a chemical fume hood. Excess APTS was removed by rinsing in distilled water. Coverslips were then activated by a 30 min incubation in 0.5% glutaraldehyde solution at room temperature, rinsed in distilled water and air-dried.

Acrylamide solutions containing either 5% or 7% w/v of a 40% acrylamide stock solution (Bio-Rad, Hercules, CA), concentrations of N,N'-methylene-bis-acrylamide ranging from 0.1% to 0.76% (Bis, 2% w/v stock solution, Bio-Rad), 35 mM HEPES, pH 8, and distilled water were prepared. The concentration of Bis was varied to control the mechanical properties of the hydrogel. As Bis concentration is increased, the elasticity of the resulting hydrogel increases. 6-((acryloyl)amino)hexanoic acid (N6) crosslinker was synthesized according to the method of Pless *et al* (1983) and co-polymerized with acrylamide (5.6 mg ml^{-1}, 20 μl N6 used in each hydrogel) and Bis in order to covalently link proteins to the surface of the hydrogel and render it adhesive to cells. Acrylamide solutions were degassed and 0.5% w/v Irgacure 2959 photoinitiator solution (Ciba, Newport, DE) was added to start polymerization.

A drop of gel solution was dispensed onto the activated side of a rectangular glass coverslip. A second Rainex-coated glass coverslip was placed on top of the gel droplet to flatten the solution, and the entire assembly was inverted and allowed to sit until beads had settled to the top surface of the gel. Gels were photopolymerized by irradiating with a 365 nm UV lamp (Ultraviolet Products, Upland, CA) for 10–15 min until the edges of the gel receded from the top coverslip. The top coverslip was gently peeled away leaving a thin gel immobilized on a rectangular glass coverslip. Gels were rinsed with ice-cold distilled water and trimmed to dimensions compatible with the main channel area of the micromachined gradient generator. Gel stiffnesses were confirmed by mechanical testing using a Q800 Dynamic Mechanical Analysis instrument (TA Instruments, New Castle, DE). Samples were dynamically compressed at a strain rate of -10% min^{-1} to a final strain of -60%. The elastic modulus of each gel sample was determined from the slope of stress and strain curves.

2.4. Determination of ligand site density by surface ELISA

Surface ELISA was used to characterize the site density of ICAM-1/Fc. 18 mm circular gels were deposited on 22 mm glass coverslips according to protocols described in section 2.3. Hydrogels were rehydrated and incubated with 200 μl 0.5 mg ml^{-1} of protein G diluted in 50 mM HEPES

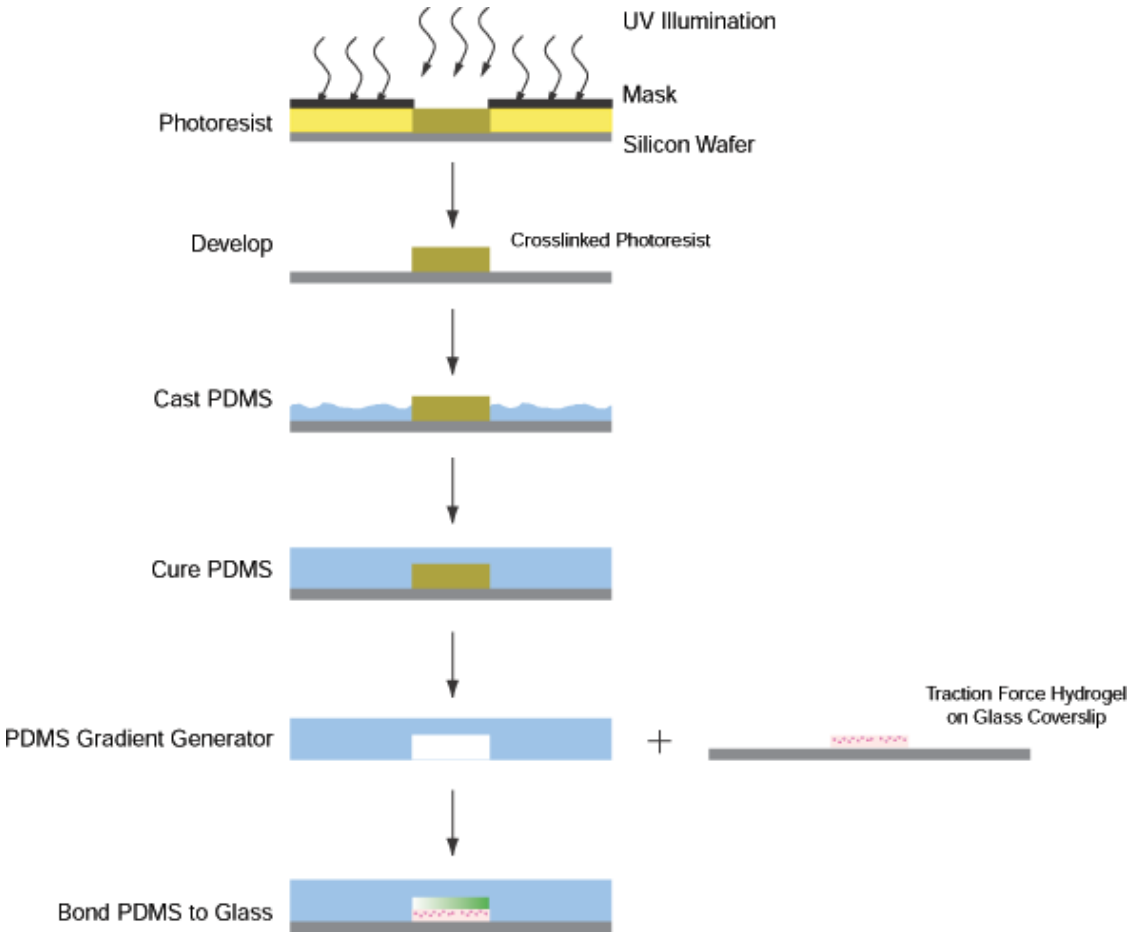

Figure 1. Fabrication of a microfluidic system to study neutrophil responses to gradients on hydrogel substrates. A schematic of the photolithography process used to prepare microfluidic devices that generate gradients over the surface of polyacrylamide hydrogels as described in section 2.

buffer, pH 6 at 4 °C for 2 h on a laboratory rocker. Hydrogels were rinsed with 0.1 M sodium bicarbonate buffer, incubated with 20 μl 50 μg ml^{-1} of ICAM-1 Fc for 2 h at room temperature on a laboratory rocker. Each hydrogel was placed in a well of a 12-well polystyrene plate. Each well was washed 3× with 2 ml ice-cold PBS. 2 ml ice-cold StartingBlock protein blocking buffer (Pierce Biotechnology) was added to each well and aspirated. Wells were washed again 3× with 2 ml ice-cold PBS. 0.9 ml of 5 μg ml^{-1} mouse anti-human ICAM-1 monoclonal ab in PBS (R&D Systems) was added to each well. Antibodies were allowed to bind for 1 h on a laboratory rocker at 4 °C. The antibody solution was aspirated and each well was washed with ice-cold PBS (2 ml, 3×). 0.9 ml of HRP rat-anti-mouse IgG monoclonal antibody (50:1 dilution in PBS, BD Pharmingen) was added to each well. The antibody allowed to bind was for 1 h on a laboratory rocker at 4 °C. Aspirated buffer and washed (2 ml PBS, 3×). Hydrogels were transferred to clean 12-well plates, and 900 μl PBS + 300 μl TMB substrate (TMB Substrate Kit, Pierce Biotechnology) was added to each well. Solutions were allowed to react for 10 min on a laboratory rocker at room temperature. The reaction was quenched with 1 ml 1N H_2SO_4. Absorbance was read on a plate reader (Tecan Infinite M200 Männedorf, Switzerland) at 450 nm. 12-well tissue culture treated polystyrene plates were used to create the calibration curve. Wells were blocked with 2 ml StartingBlock then washed with 3 ml PBS per well 4×. 900 μl HRP biotin was added to wells at concentrations between 0 and 0.003 μg ml^{-1}. 300 μl TMB substrate was added to each well. Reactions were allowed to proceed 10 min on a laboratory rocker at room temperature. Reactions were then quenched with 1 ml 1N H_2SO_4. Then we read the absorbance on a plate reader at 450 nm.

2.5. Fabrication and assembly of microfluidic flow chambers

Gradient generating microfluidic networks were designed according to principles described by Dertinger and Whitesides (Dertinger *et al* 2001). Microfluidic chambers used in this study were fabricated by bonding PDMS chips (Sylgard 184, Dow Corning, Midland, MI) to glass coverslips as described previously (Li Jeon *et al* 2002). PDMS chips were prepared from silicon wafer templates using photolithography as shown in figure 1. A negative master template was prepared by depositing a thick film of SU8 photoresist (MicroChem, Boston, MA) onto the surface of a clean 3 in silicon wafer. The photoresist film was patterned by exposure to UV light through a high resolution negative transparency mask in a Karl Suss mask aligner. After exposure, uncrosslinked regions

of the wafer were developed away, leaving a raised network of channels on the surface of the wafer. PDMS chips with embedded channels were prepared by pouring a 10:1 ratio of PDMS polymer to cross-linking agent onto the silicon template, degassing and curing in an oven for 1 h at 80 °C. Cured PDMS chambers were cut out and peeled away from the template wafer. Inlet and outlet ports were punched into the chambers using a 20 gauge blunt end needle.

To permanently seal PDMS chambers to glass coverslips containing immobilized hydrogels, PDMS and glass surfaces were briefly exposed to reactive oxygen plasma under vacuum. The main channel of the microfluidic device was aligned with the hydrogel substrate on the glass coverslip, and the surfaces were pressed into contact. Hydrogels within assembled microfluidic devices were rehydrated and incubated with 0.5 mg ml^{-1} of protein G diluted in 50 mM HEPES buffer, pH 6 at 4 °C. Hydrogels were rinsed with 0.1 M sodium bicarbonate buffer, incubated with 50 μg ml^{-1} of ICAM-1 Fc and 50 μg ml^{-1} of E-Selectin Fc at room temperature, and used immediately after incubation was complete. Each assembled microfluidic device was used once.

2.6. Operation of microfluidic flow chambers

Assembled microfluidic devices were vacuum-filled according to the method of Monahan and colleagues (2001) and connected to syringes filled with chemoattractant gradient solutions. Gradient solutions were pumped through the device using an infusion/withdrawal syringe pump (Harvard Apparatus, South Natick, MA) set up inside a heated microscope stage with temperature controlled at 37 °C. Flowrates of each gradient solution were controlled throughout the duration of an experiment, resulting in a wall shear stress of less than 1 dyne cm^{-2}. The spatial profile of the gradient was tracked during experiments by monitoring the fluorescent intensity of fluorescein dye introduced at different concentrations into each gradient solution. Once fMLP gradients were established, cells were loaded into the microfluidic chamber through a dedicated side inlet port. Neutrophils captured from free stream flow rolled along the surface of the gel and became firmly adherent.

2.7. Cell tracking and quantitation of motility

The positions of firmly adherent cells at different positions within the chamber were captured using a Nikon Inverted Eclipse TE300 microscope with a Nikon 20×, numerical aperture 0.40, objective. Time-lapse images were recorded at 30 s intervals for a minimum of 15 min. The position of cell centroids at each time interval was determined using ImageJ software. Mean-squared displacements for the centroids of each cell were calculated and used to determine individual cell speed. In the presence of linear gradients within the microfluidic chamber, the chemotactic index was calculated by measuring the distance traveled in the direction of the gradient divided by the total path length. Data from individual cells was averaged to obtain a single value for each parameter and experimental condition evaluated.

2.8. Traction force microscopy

Traction force microscopy was performed as described previously on firmly adherent neutrophils within the microfluidic chamber using a Nikon Inverted Eclipse TE300 microscope with a Nikon 100×, numerical aperture 1.30 oil objective (Reinhart-King *et al* 2003, Smith *et al* 2007). A phase contrast and corresponding fluorescent bead image were captured simultaneously for each cell at different time intervals. At the end of each experiment, cells were detached from the hydrogel by addition of a 1 M EDTA or 0.25% trypsin-EDTA solution, and an image of the unstressed field of view was taken. Traction forces were determined based on deformations of the hydrogel substrate reported by the motion of fluorescent beads embedded within the top surface. Using custom-written LIBTRC 2.0 software, bead displacements within the gel were calculated and the most likely surface traction vectors were obtained as described by Dembo and Wang (Dembo and Wang 1999). The overall force $|F|$ exerted by the cell on the substrate is an integral of the traction stress over the cell contact region, $|F| = \int\int \sqrt{T_x^2(x,y) + T_y^2(x,y)}\,dx\,dy$, where $T(x,y) = [T_x(x,y), T_y(x,y)]$ is the continuous field of traction vectors defined at any spatial position (x, y) within the contact region.

3. Results

3.1. Neutrophil spreading and adhesion depend on hydrogel mechanics

To investigate the spreading and adhesion of neutrophils on hydrogels in response to spatially and temporally controlled chemical cues, a microfluidic gradient generator was fabricated as described in figure 1. Cells were perfused into chambers, allowed to adhere to the surface of the hydrogel and exposed to a range of well-defined adhesive, chemical and mechanical conditions (figure 2). Stable chemical gradients were generated over hydrogels with shear moduli ranging from 300 Pa (soft) to 12 000 Pa (stiff). The values of hydrogel moduli tested in our studies encompass the range of tissue mechanics that a neutrophil could encounter *in vivo* (Paszek *et al* 2005, Engler *et al* 2006). Surface ELISA experiments proved that changes in hydrogel modulus do not significantly affect the ligand site density; results for experiments on two hydrogels (2.5 and 31.2 kPa), which represent the range of stiffnesses investigated in this work, are shown in figure 3. These two hydrogels were tested because any change in ligand site resulting from increased concentrations of Bis in the hydrogel would be most evident in these samples. Three independent measurements were made for each gel. These tests show that some variability exists from hydrogel to hydrogel because site density is a function of both protein G and ICAM-1 Fc orientation, a parameter that we expect to have some natural variability. Ligand density on both hydrogels is of the same order of magnitude, and a t-test performed on the ELISA data, using $\alpha = 0.05$, resulted in p-value $= 0.36$, which further supports the claim that ligand density is not correlated to hydrogel stiffness. Furthermore, any site density variability is

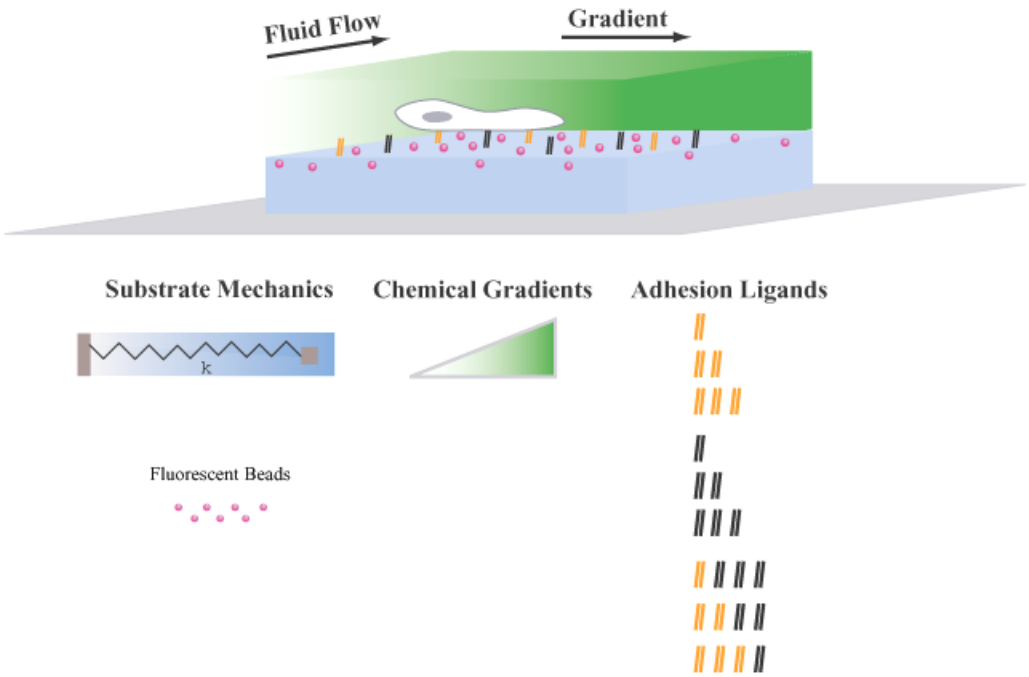

Figure 2. Schematic representation of an adherent neutrophil on a hydrogel within a microfluidic gradient chamber. A single cell is shown interacting with a ligand-coated surface oriented in the direction of increasing chemical gradient. Ligands are immobilized on the surface of the hydrogel via covalent bonds as described in section 2. The direction of fluid flow as well as chemical and mechanical parameters within the system that can be varied independently of each other are also illustrated.

random with respect to the entire population of hydrogels used. To understand the influence of substrate mechanics on cell spreading, neutrophils were activated with a uniform solution of 10 nM fMLP and imaged with time-lapse microscopy. As shown in figure 4(a), the time-averaged spreading area of neutrophils on hydrogels with constant ligand density increased as the underlying substrate modulus was increased. Neutrophils placed on stiff 12 kPa hydrogel surfaces deformed and flattened extensively across the surface generating large spread areas. Spreading on the softer surfaces was much less pronounced. The difference in cell area between the 12 kPa and 300 Pa hydrogel conditions evaluated was approximately 3–4 fold.

The difference in time-averaged cell spreading area on different hydrogel stiffnesses can be explained by two separate observations. Figures 4(b) and (c) show that the initial spread area of a neutrophil just after activation on softer gels is less than that of a cell on a stiff gel. The cell area on the soft gel decreases even further over the span of 10 min. After 10 min, the neutrophil on the soft hydrogel appears white in phase contrast microscopy, indicating its morphology has become more round and the cell body is no longer in the same focal plane as the hydrogel (figure 4(b)). Although neutrophils undergo a transition to a rounder morphology on soft gels over time, they remain viable and continue to migrate. Graphs of cell area over time confirm the trend observed by microscopy. Measurements of individual cell areas for a particular gel stiffness plotted as a function of time show that cell adhesion and spreading area is stabilized on stiff 12 kPa gels, but decreases as a function of time when the hydrogel stiffness is decreased (figure 4(d)). To quantify this observation, the time at which cell area decreased by 50% for a particular gel stiffness was determined (figure 4(e)). On soft gels (<7000 Pa), interactions between the neutrophil and hydrogel substrate lead to a significant decrease in spread area in less than 5 min.

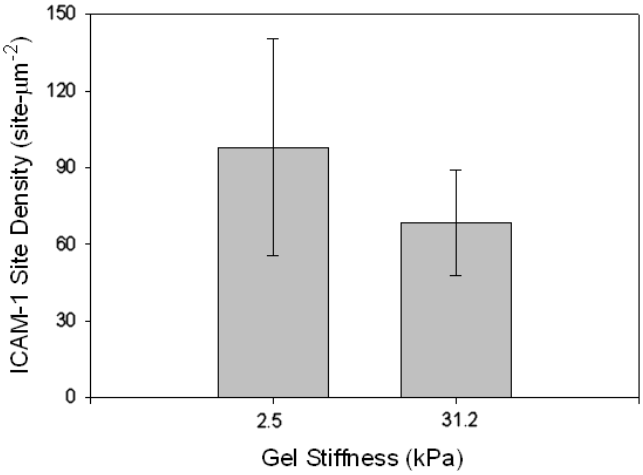

Figure 3. ICAM-1 Fc site densities on different stiffness hydrogels determined by surface ELISA. Surface ELISA experiments (described in section 2) on hydrogels of different moduli coated with equal concentrations of ICAM-1 Fc show that hydrogel stiffness can be adjusted independent of ligand site density. This data is based on three independent measurements for each hydrogel reported, and the error bars are based on SD. Furthermore, a t-test was performed using $\alpha = 0.05$ which resulted in p-value $= 0.36$. This result further indicates that ligand densities on these two gels are not statistically different.

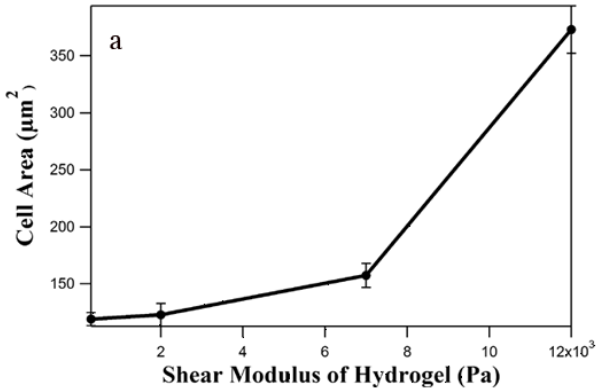

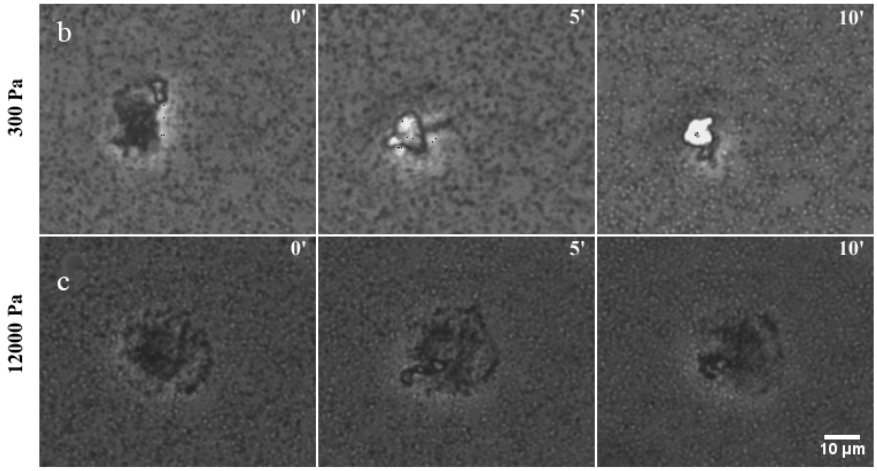

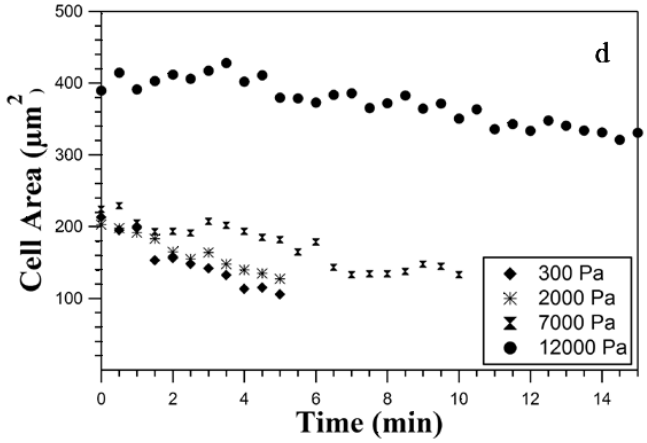

e

G (Pa)	$t_{1/2}$ (min)
300	4.81
2000	6.52
7000	11.61
12000	34.36

Figure 4. Neutrophil adhesion and spreading on hydrogels depends on substrate mechanical properties. (a) Neutrophils were activated with 10 nM fMLP and observed during adhesion to hydrogel substrates. The area of individual cells attached to a hydrogel during a 15 min time interval was averaged and plotted against hydrogel shear modulus to show the influence of substrate mechanics on cell spreading. Error bars represent the SEM of 11–20 cells. ((b), (c)) Phase contrast images of neutrophils adhering to hydrogel surfaces in uniform solutions of 10 nM fMLP on soft (300 Pa) and stiff (12 kPa) gels as a function of time. (d) Cell area of neutrophils activated with uniform solutions of 10 nM fMLP on hydrogels at the indicated stiffnesses were measured and plotted as a function of time. Each timepoint represents an average of 15 cells. (e) The time at which cell spreading area for a given hydrogel stiffness had decreased by 50%.

3.2. Sensitivity of chemotactic response depends on hydrogel stiffness

We used time-lapse microscopy to observe neutrophil motility in response to varying fMLP cues on hydrogels of varying stiffness. Figure 5 shows the initial and final positions of several cells migrating in response to a uniform stimulus of 10 nM fMLP (a) or a gradient of fMLP of 10 nM/10 μm (b). The data shows that cells on the softest gel in 10 nM uniform fMLP are weakly adherent and migration is biased in

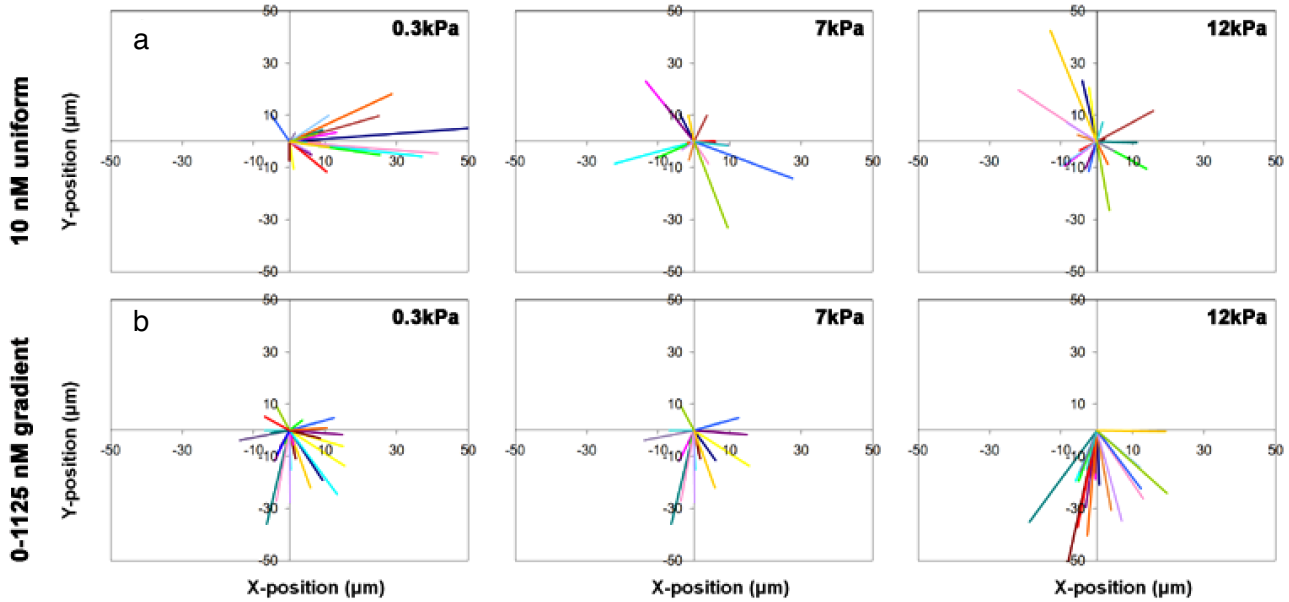

Figure 5. Neutrophil trajectories during chemokinesis or chemotaxis on hydrogels with varying mechanical properties. Representative 2D Wind–Rose plots showing individual cell trajectories for a range of gel stiffnesses in both uniform (a) and gradient (b) solutions of fMLP ($n = 11$–20). After cells are imaged using time-lapse microscopy, centroids are computed and individual cell tracks are generated. Trajectories were obtained by tracking cell centroids for a total time of 15 min per condition. Lines begin at the zero-centered initial position of each cell and end at the final position to display net cell dispersion. For each graph with a gradient, the spatial gradient of fMLP increases from top to bottom.

the direction of marginal flow in the chamber (left to right). When stimulated with a gradient of fMLP, cell migration on the 0.3 kPa gel still appears random, although it is no longer biased in the direction of fluid flow. At an intermediate gel stiffness of 7 kPa, cell motility appears random in response to a uniform concentration of 10 nM fMLP and becomes somewhat more directed in the presence of a gradient (10 nM/10 μm). Lastly, on the stiff 12 kPa gel, cell motility is random in response to uniform 10 nM fMLP stimulation and becomes highly directed in response to stimulation with a gradient. These results show that neutrophils are capable of responding more strongly to a chemical gradient on stiffer hydrogels compared to neutrophils interacting with softer substrates.

To further quantify the differences observed in neutrophil trajectories on hydrogels of varying matrix rigidity, migration parameters such as speed and chemotactic index were measured. The chemotactic index is defined as the distance a neutrophil travels in the direction of increasing gradient divided by the total distance traveled (Lauffenburger and Linderman 1993). Therefore, the chemotactic index ranges from zero to one and is an index of cell directionality. As shown in figures 6(a) and (c), neutrophils are highly motile on hydrogels over a range of stiffnesses during chemokinesis and chemotaxis. As expected, the chemotactic index during chemokinesis (10 nM) is approximately zero for all hydrogel stiffnesses (figure 6(b)). In contrast, significant increases in the chemotactic index are observed with stiffer gels in a chemotactic gradient (10 nM/10 μm). On soft hydrogels (0.3 kPa), the chemotactic index in a gradient is only slightly higher than cells in the presence of uniform 10 nM fMLP. The results observed on the stiff gel compare well to previous reports of changes in the chemotactic index in neutrophils in response to different gradients on glass (Herzmark *et al* 2007). Both observations of cell trajectories and calculated migration parameters show that changes in hydrogel mechanics influence a neutrophil's response to stimulation with fMLP gradients.

We also determined how changes in substrate stiffness affect the spatial distribution of forces. As shown previously, we find that on stiff hydrogels the highest traction forces are located at the rear of the cell relative to motion (figures 7(a) and (b)) (Smith *et al* 2007). Using TFM analysis, we show that, on most gel materials, directed motion is driven by punctate, discrete force centers in the uropod. As hydrogel stiffness is decreased, a corresponding decrease in the intensity and spatial area of these regions of high stress within the cell at the rear is observed. At the lowest gel stiffness, the traction stress map displays only a small region of high force that is no longer oriented at the rear of the cell with respect to motion or the external fMLP gradient (figure 7(e)). The stress maps illustrate that a steep chemotactic gradient results in an asymmetric distribution of traction forces in neutrophils on stiff gel substrates and that decreased force asymmetry is observed on softer gels.

3.3. Effect of hydrogel stiffness on neutrophil chemotaxis

Because the fMLP gradient used in figure 6 resulted in both a high mean concentration of fMLP and a high gradient steepness (C_m = 10 nM, slope = 10 nM/10 μm), we set out to determine whether the effect of substrate modulus on chemotactic sensitivity of neutrophils would be altered if cells were stimulated with the same gradient but with different mean fMLP concentrations that span the K_d of the receptor, or with a

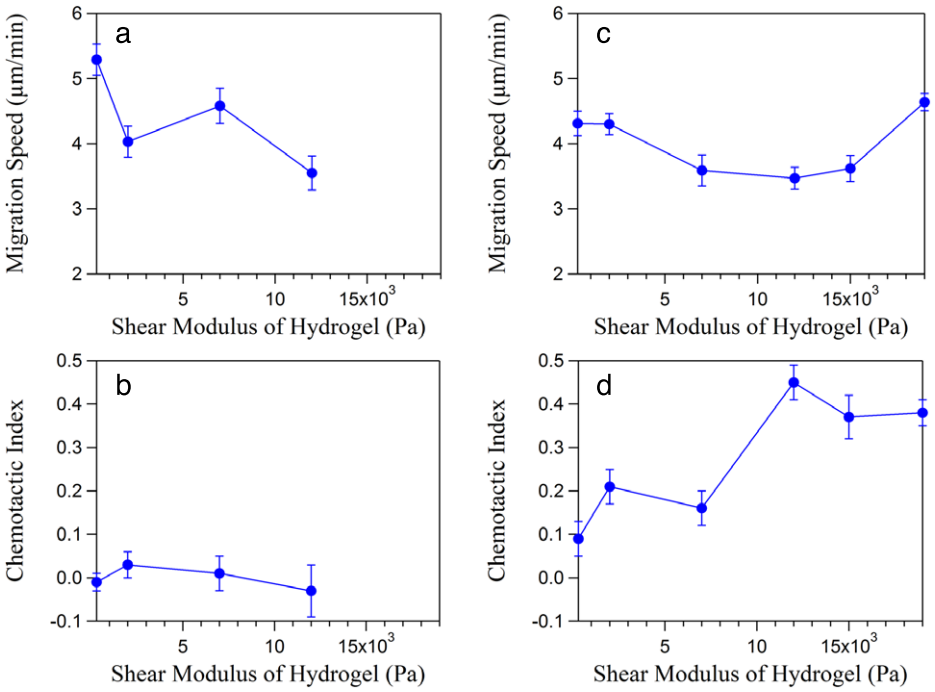

Figure 6. Relationship between cell speed and directionality as a function of hydrogel stiffness. Migration parameters for neutrophils obtained on hydrogels functionalized with ICAM-1/E-Selectin in the presence of uniform or gradient solutions of fMLP. (a) Migration speed, (b) chemotactic index in a uniform concentration of 10 nM fMLP. (c) Migration speed, (d) chemotactic index in a gradient of 0–1125 nM fMLP or 10 nM/cell diameter (10 nM/10 μm). For each hydrogel stiffness in a uniform concentration of fMLP, error bars represent the SEM of $n = 20$ cells ((a), (b)). For gradient solutions, error bars represent the SEM of $n = 11$–20 cells ((c), (d)).

shallower gradient. Such precise control of the fMLP gradient is made possible by our micromachined chamber. Previous work has demonstrated that, when cells are in a gradient, fMLP concentrations near the receptor K_d produce maximal migration responses (Zigmond 1977). The K_d of the fMLP receptor is known to be approximately 10 nM (Herzmark *et al* 2007). We therefore examined four equivalent gradients of fMLP with different C_m by examining different subregions of a hydrogel within a microfluidic gradient of 0–56.25 nM set over a channel width of 1125 μm. This produced a gradient of 0.5 nM μm^{-1} or 5 nM/10 μm. The response of the chemotactic index for each gradient and mean concentration were quantified for five different gel stiffnesses ranging from 300 Pa to 19 kPa (figure 8). The basic trend that the CI increases with increasing gel stiffness is maintained at all values of C_m. As the mean concentration is increased to 35 nM and above for a gradient slope of 0.5 nM/cell diameter, the effect of mechanics on chemotactic sensitivity becomes less pronounced, but only because chemotaxis is itself decreased because of receptor saturation. Because fMLP receptor binding is saturable, receptor occupancy is less sensitive to the gradient of chemoattractant when the mean concentration is high.

In addition to considering the potential effect of the mean concentration of fMLP, we also examined the possibility that the observed effect of substrate modulus on chemotaxis was simply due to a change in cell size that affected the length scale over which gradient sensing could occur. To determine whether the decrease in cell radius on soft gels explained the reduced chemotactic sensitivity, we normalized the measured chemotactic index on each gel stiffness from figure 6(d) (C_m = 100 nM, slope = 10 nM/10 μm) to cell radii obtained from cell spreading data (figure 4). As shown in figure 9, accounting for changes in cell radii does not change the trend we report in figure 6(d). Our analysis suggests that simple changes in cell geometry are not sufficient to account for the decrease in chemotaxis that we observe on softer gels.

3.4. Neutrophil integrin requirements during chemotaxis depend on substrate stiffness

Because neutrophil migration on glass and plastic surfaces is known to be mediated by integrin receptors and because integrins are responsive to changes in substrate mechanics, and because we functionalized our surfaces with the β2-integrin ligand ICAM-1, we examined requirements for integrin receptor usage during neutrophil migration on hydrogels functionalized with ICAM-1 (Woolf *et al* 2007, Choquet *et al* 1997). Similar to 2D results on glass and plastic surfaces, we find that blocking integrins with a widely used β2 integrin antibody (TS1/18) reduces cell spreading on both soft (2 kPa) and stiff (12 kPa) gels (figure 10). Surprisingly, integrin inhibition does not significantly affect cell speed on either soft or stiff substrates. For neutrophils migrating on stiff gels, a significant decrease in the chemotactic index is observed, while the chemotactic index of cells on soft gels remains the same. Migration parameters of neutrophils on soft (2 kPa) gels appear to be unaffected by integrin blocking. This suggests that neutrophils on soft gels may not employ or activate β2 integrins to the same degree as that observed on the stiff gels.

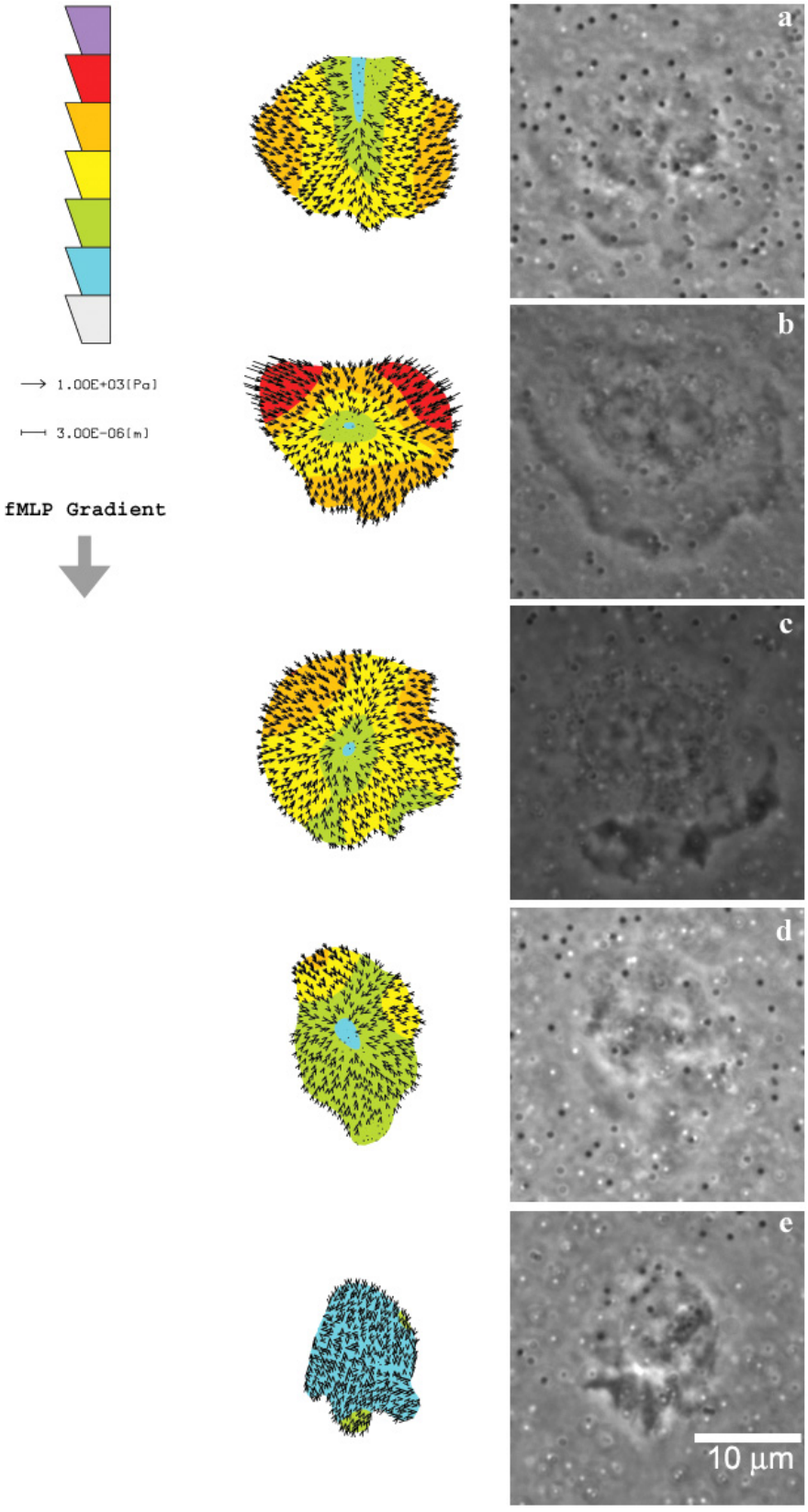

Figure 7. Traction stress maps of neutrophils migrating on hydrogels of varying stiffness in response to a gradient of fMLP. Neutrophil traction stress maps and corresponding phase contrast images during migration on stiff hydrogels (12 000 Pa) in response to a gradient of fMLP (10 nM/cell diameter). Arrow pointing downwards indicates the direction of the fMLP gradient from low to high concentration within the microfluidic chamber. Color map indicates the magnitude of stress in different regions of the cell. Horizontal arrow indicates the magnitude of the force vectors drawn within each cell.

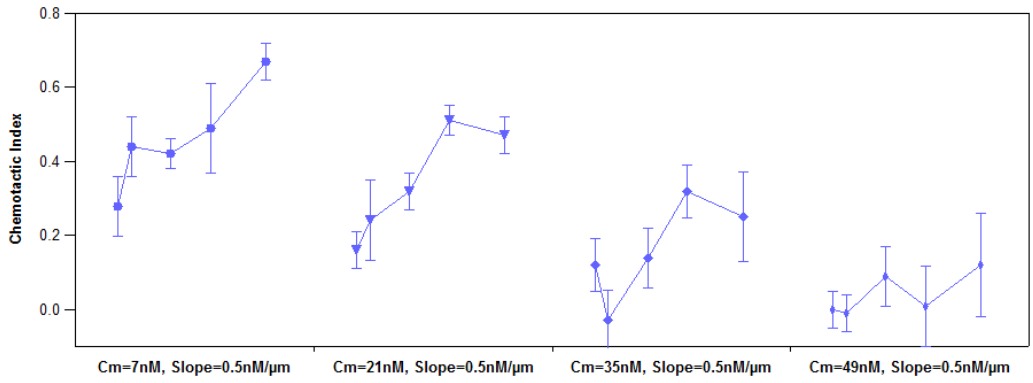

Figure 8. Chemotaxis in linear fMLP gradients with varying mean concentrations as a function of hydrogel stiffness. Neutrophil chemotaxis in linear fMLP gradients with mean concentrations ranging between 7–49 nM and constant slope was measured on hydrogels with shear moduli of 300, 2000, 7000, 12 000 and 19 000 Pa. For each line, shear modulus increases from left to right. Error bars represent the SEM of $n = 10$ cells.

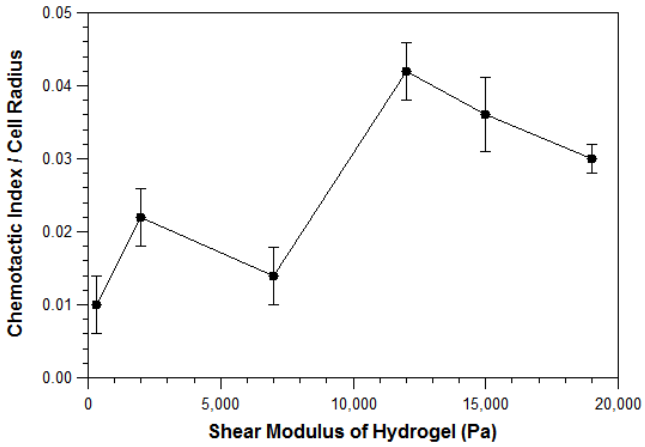

Figure 9. Chemotactic index values for neutrophils on hydrogels of varying stiffness normalized to observed cell radius. To account for differences in spatial gradient sensing that would result from changes in cell spreading, chemotactic index values were replotted after normalization to average cell radii observed on different gel stiffnesses. The cell radii was used as the characteristic length for normalization because spatial sensing occurs across a cell's diameter.

4. Discussion

In this study, we measured neutrophil chemokinesis and chemotaxis on hydrogel materials under well-defined chemoattractant gradients imposed upon the cell in a micromachined gradient chamber. We believe we are the first to combine these two methodologies; most often, chemotaxis on hydrogels has been measured by releasing chemoattractants from a pipette (Smith *et al* 2007, Oakes *et al* 2009). As a result, we are able to understand the relationship between the magnitude and steepness of the chemoattractant gradient and directed cell motility on hydrogels.

We have observed that neutrophil migration is strongly dependent on shear modulus of the gel. In a chemotactic gradient, varying gel stiffness from 300–12 000 Pa can switch motility from random to directed, simply due to changes in hydrogel mechanics. This result largely corresponds to that shown previously by Oakes *et al* (2009). This observation suggests that a neutrophil has a mechanism for tactile sensing that enables it to distinguish between mechanical environments based on stiffness. To identify how such a mechanism might work, we show that a neutrophil first responds to substrates by spreading and exploring the mechanics of the substrate. In the initial stage of spreading, active integrins on the cell surface are required. After initial spreading has occurred, further spreading and the lifetime of adhesion depend on the ability of a neutrophil to generate tension against the substrate through contractility. Apparently because of the requirement for high internal tension, complete spreading and adhesion stabilization is observed only on stiff gels. If the level of tension that is loaded via integrins during the contractile phase of spreading is insufficient, the neutrophil reduces its adhesive area as we observed. The data suggests that a neutrophil possesses tactile machinery that it can use to probe its underlying substrate and to modulate its adhesiveness and tension on a timescale of minutes, consistent with the rapid motility and dynamics of these cells. Anchorage-dependent cells probe their substrates through focal adhesion assemblies that can take hours to form and subsequently generate adhesive responses that occur on similar timescales (Zhang *et al* 2008). Our work suggests that neutrophil spreading involves two different stages, an initial expansion/contact phase and a contraction phase. Similar results have been observed for other cell types that lack focal adhesion machinery (Zhang *et al* 2008, Fleire *et al* 2006). The contraction phase likely depends on outside-in signaling through integrins and myosin II and is responsible for prolonged, stable spreading.

Changes in neutrophil adhesion that we observe on hydrogels are reflected in changes of migration dynamics. We have shown that the ability of a cell to move directionally up a gradient is strongly dependent on substrate stiffness, as was shown previously (Oakes *et al* 2009). We further observed that substantial changes in the chemotactic index are accompanied by avid force generation but without significant changes in speed, and that the magnitude of traction stress were much greater on stiffer gels and concentrated in discrete force centers in the uropod of the cell; these results seem to be in conflict with those presented previously (Oakes *et al* 2009). Our current view is that contractile punctate force centers lead to a hydrodynamic squeezing at the tail

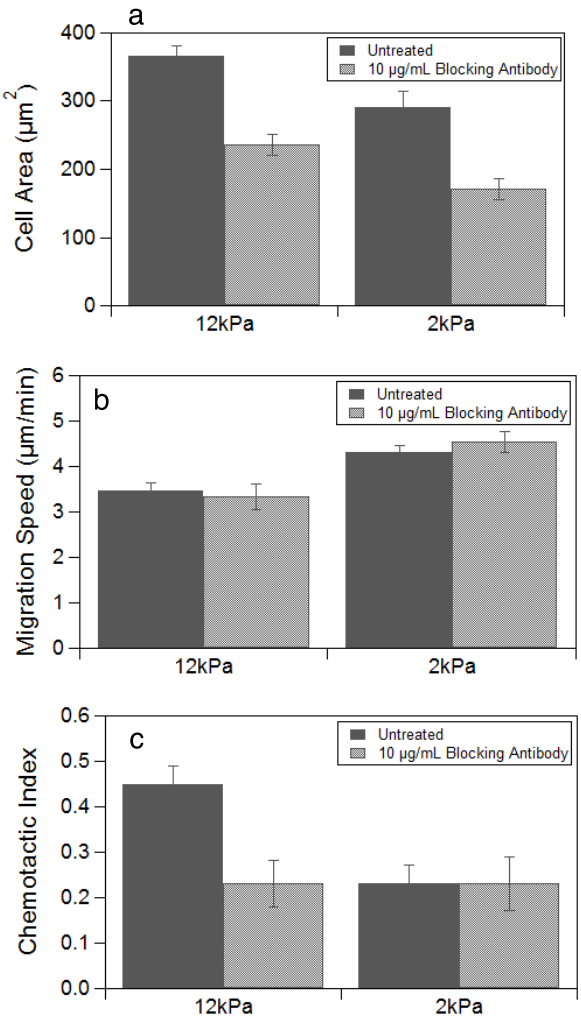

Figure 10. Effect of $\beta 2$ integrin blocking antibody. Neutrophils were incubated with 10 μg ml^{-1} TS1/18 antibody and allowed to attach and migrate on either soft (300 Pa) or stiff (12 000 Pa) hydrogels in the presence of a 0–1125 nM gradient (10 nM/10 μm). (a) Cell spreading, (b) migration and (c) chemotactic index were measured for individual cells tracked for a total of 15 min. Error bars represent the SEM of $n = 20$ cells.

that propels the cytoplasm and the leading edge forward, much in the manner that toothpaste is squeezed from a tube. Because we employed a micromachined gradient chamber, we uniquely were able to correlate directional motion with gradient steepness, mean concentration and substrate elasticity. We find that our persistence measure is always maximal when the mean chemoattractant concentration is close to the K_d of binding of the fMLP receptor for a given gradient steepness. Further, for a given set of chemotactic parameters, increasing stiffness led to an increasing directional response. However, increasing substrate stiffness was simply a facilitating factor and did not enable a neutrophil to respond to a gradient at very high mean concentrations when all its receptors are saturated. These insights could be uniquely elucidated using our experimental technique.

It is interesting that the ability of a cell to generate speed and to migrate directionally up a linear chemical gradient appear to be separate processes. Because neutrophil morphology and spreading are different on soft and stiff surfaces and because the cells show different requirements for integrins depending on stiffness, it is possible that a neutrophil is capable of switching seamlessly between two different strategies for motility. In the first mode of migration, a high level of cell spreading and tension through integrins is required. In the second mode, migration depends less on integrins and a higher degree of blebbing extensions are observed.

We considered the possibility that changes in chemotactic sensitivity across gel mechanics could simply be due to decreases in cell radius that in turn lead to reduced gradient sensing capability. This type of mechanism has been reported for anchorage-dependent cells (Meyers *et al* 2006, Neves *et al* 2008). However, normalizing the chemotactic index obtained across a range of hydrogel stiffnesses to the corresponding cell radius does not affect the trend of the data. Further, lowering the mean fMLP concentration to values approximately equal to the receptor K_d, where gradient sensing should be most sensitive, produces the same strong dependence of motility on gel stiffness. Although we observe that neutrophil migration on soft gels is less directed in two dimensions, it is possible that the formation of membrane extensions directed towards a gradient coupled with low integrin adhesiveness in constrained 3D tissue environments could lead to different results.

Lastly, numerous papers have reported the requirements for integrin receptors during cell motility (Palecek *et al* 1997, Zaman *et al* 2006). This notion has recently been challenged by Lammermann *et al* (2008) who show that pan-integrin deficient neutrophils are also capable of motility *in vivo* (Lammermann *et al* 2008). In addition, Woolf and Alon show that T-cells which share the same integrin receptors as neutrophils are capable of undergoing motility responses in the absence of integrin adhesiveness using the same blocking antibody we employ (Woolf *et al* 2007). Two explanations are proposed for this behavior in prior work. The first is that neutrophils only require integrins for migration in two dimensions, and that integrins are not required for motion in three dimensions. Second, depending on how integrin adhesiveness is regulated for a specific cell type, chemical signals in certain environments may silence integrin activation. Our work on 2D hydrogel substrates shows there are integrin-dependent and integrin-independent modes of motility. Based on our work, we hypothesize that simple changes in mechanics that occur between 2D glass and plastic surfaces as compared to soft 3D hydrogels that are commonly used may help to explain some of the differences observed in immune cell motility behavior between these two different *in vitro* systems.

An interesting speculation of this work is that neutrophils should crawl more avidly toward a target when the substrate stiffens. Since neutrophils must move very quickly from the endothelial apical surface to the extracellular matrix, a gradient in elasticity might accelerate extravasation. If some or all integrins are not required for neutrophil migration in softer mechanical compartments *in vivo*, such as the interstitial space where chronic inflammation and accumulation of inflammatory cells typically occurs, then inhibition of integrins would not represent an optimal targeting strategy for inflammatory

disease. Indeed, many of the integrin inhibitors targeting inflammation tested in humans have met with limited or little success (Staunton *et al* 2006, Yonekawa and Harlan 2005). Moreover, due to the plasticity in integrin use by neutrophils and other immune cells, a more effective strategy for targeting migration in inflammation would be to apply inhibitors of integrin and integrin-independent motility in parallel. We provide here results of the first quantitative study of neutrophil responses to substrate mechanics in well-defined chemotactic gradients.

Acknowledgments

We thank Eric Johnston for helpful discussions. This work was supported by National Institutes of Health grants HL18208 and HL08533 and Fellowships from Merck to RAJ and BGR.

References

Alon R and Ley K 2008 Cells on the run: shear-regulated integrin activation in leukocyte rolling and arrest on endothelial cells *Curr. Opin. Cell Biol.* **20** 525–32

Balaban N Q *et al* 2001 Force and focal adhesion assembly: a close relationship studied using elastic micropatterned substrates *Nat. Cell Biol.* **3** 466–72

Beningo K A, Dembo M, Kaverina I, Small J V and Wang Y L 2001 Nascent focal adhesions are responsible for the generation of strong propulsive forces in migrating fibroblasts *J. Cell. Biol.* **153** 881–8

Chen C E and Odde D J 2008 Traction dynamics of filopodia on compliant gels *Science* **322** 1687–91

Choquet D, Felsenfeld D P and Sheetz M P 1997 Extracellular matrix rigidity causes strengthening of integrin-cytoskeleton linkages *Cell* **88** 39

Dembo M and Wang Y L 1999 Stresses at the cell-to-substrate interface during locomotion of fibroblasts *Biophys. J.* **76** 2307–16

Dertinger S K W, Chiu D T, Jeon N L and Whitesides G M 2001 Generation of gradients having complex shapes using microfluidic networks *Anal. Chem.* **73** 1240–6

Devreotes P N and Zigmond S H 1988 Chemotaxis in eukaryotic cells—a focus on leukocytes and dictyostelium *Annu. Rev. Cell Biol.* **4** 649–86

Engler A J, Sen S, Sweeney H L and Discher D E 2006 Matrix elasticity directs stem cell lineage specification *Cell* **126** 677–89

Fleire S J, Goldman J P, Carrasco Y R, Weber M, Bray D and Batista F D 2006 B cell ligand discrimination through a spreading and contraction response *Science* **312** 738–41

Giannone G and Sheetz M P 2006 Substrate rigidity and force define form through tyrosine phosphatase and kinase pathways *Trends Cell Biol.* **16** 213–23

Gupton S L and Waterman-Storer C M 2006 Spatiotemporal feedback between actomyosin and focal-adhesion systems optimizes rapid cell migration *Cell* **125** 1361–74

Herzmark P, Campbell K, Wang F, Wong K, El-Samad H, Groisman A and Bourne H R 2007 Bound attractant at the leading versus the trailing edge determines chemotactic prowess *Proc. Natl Acad. Sci.* **104** 13349–54

Jannat R A 2009 Quantitative analysis of immune cell motility and mechanics on hydrogel substrates *Bioengineering* (Philadelphia, PA: University of Pennsylvania)

Lammermann T *et al* 2008 Rapid leukocyte migration by integrin-independent flowing and squeezing *Nature* **453** 51–5

Lauffenburger D A and Linderman J J 1993 *Receptors: Models for Binding, Trafficking, and Signaling* (New York: Oxford University Press)

Li Jeon N, Baskaran H, Dertinger S K, Whitesides G M, Van de Water L and Toner M 2002 Neutrophil chemotaxis in linear and complex gradients of interleukin-8 formed in a microfabricated device *Nat. Biotechnol.* **20** 826–30

Lo C M, Wang H B, Dembo M and Wang Y L 2000 Cell movement is guided by the rigidity of the substrate *Biophys. J.* **79** 144–52

Lombardi M L, Knecht D A, Dembo M and Lee J 2007 Traction force microscopy in dictyostelium reveals distinct roles for myosin II motor and actin-crosslinking activity in polarized cell movement *J. Cell Sci.* **120** 1624–34

Meyers J, Craig J and Odde D J 2006 Potential for control of signaling pathways via cell size and shape *Curr. Biol.* **16** 1685–93

Monahan J, Gewirth A A and Nuzzo R G 2001 A method for filling complex polymeric microfluidic devices and arrays *Anal. Chem.* **73** 3193–7

Munevar S, Wang Y L and Dembo M 2001a Distinct roles of frontal and rear cell-substrate adhesions in fibroblast migration *Mol. Biol. Cell* **12** 3947–54

Munevar S, Wang Y L and Dembo M 2001b Imaging traction forces generated by migrating fibroblasts *Biophys. J.* **80** 1744–57

Neves S R *et al* 2008 Cell shape and negative links in regulatory motifs together control spatial information flow in signaling networks *Cell* **133** 666–80

Oakes P W, Patel D C, Morin N A, Zitterbart D P, Fabry B, Reichner J S and Tang J X 2009 Neutrophil morphology and migration are affected by substrate elasticity *Blood* **114** 1387–95

Palecek S P, Loftus J C, Ginsberg M H, Lauffenburger D A and Horwitz A F 1997 Integrin-ligand binding properties govern cell migration speed through cell-substratum adhesiveness *Nature* **385** 537–40

Paszek M J, Boettiger D, Weaver V M and Hammer D A 2009 Integrin clustering is driven by mechanical resistance from the glycocalyx and the substrate *PLoS Comput. Biol.* **5** e1000604

Paszek M J *et al* 2005 Tensional homeostasis and the malignant phenotype *Cancer Cell* **8** 241–54

Pelham R J and Wang Y L 1997 Cell locomotion and focal adhesions are regulated by substrate flexibility *Proc. Natl Acad. Sci. USA* **94** 13661–5

Peyton S R and Putnam A J 2005 Extracellular matrix rigidity governs smooth muscle cell motility in a biphasic fashion *J. Cell. Physiol.* **204** 198–209

Pless D D, Lee Y C, Roseman S and Schnaar R L 1983 Specific cell adhesion to immobilized glycoproteins demonstrated using new reagents for protein and glycoprotein immobilization *J. Biol. Chem.* **258** 2340–9

Puklin-Faucher E, Gao M, Schulten K and Vogel V 2006 How the headpiece hinge angle is opened: new insights into the dynamics of integrin activation *J. Cell Biol.* **175** 349–60

Reinhart-King C A, Dembo M and Hammer D A 2003 Endothelial cell traction forces on RGD-derivatized polyacrylamide substrata *Langmuir* **19** 1573–9

Reinhart-King C A, Dembo M and Hammer D A 2005 The dynamics and mechanics of endothelial cell spreading *Biophys. J.* **89** 676–89

Reinhart-King C, Dembo M and Hammer D A 2008 Cell–cell mechanical communication through compliant substrates *Biophys. J.* **95** 6044–51

Simon S I and Green C E 2005 Molecular mechanics and dynamics of leukocyte recruitment during inflammation *Annu. Rev. Biomed. Eng.* **7** 151–85

Smith L A, Aranda-Espinoza H, Haun J B, Dembo M and Hammer D A 2007 Neutrophil traction stresses are concentrated in the uropod during migration *Biophys. J.* **92** L58–60

Staunton D E, Lupher M L, Liddington R and Gallatin W M 2006 Targeting integrin structure and function in disease *Advances in Immunology* vol 91 (San Diego, CA: Elsevier Academic) pp 111–57

Tranquillo R T, Lauffenburger D A and Zigmond S H 1988 A stochastic-model for leukocyte random motility and chemotaxis based on receptor-binding fluctuations *J. Cell Biol.* **106** 303–9

Woolf E, Grigorova I, Sagiv A, Grabovsky V, Feigelson S W, Shulman Z, Hartmann T, Sixt M, Cyster J G and Alon R 2007 Lymph node chemokines promote sustained T lymphocyte motility without triggering stable integrin adhesiveness in the absence of shear forces *Nat. Immunol.* **8** 1076

Yonekawa K and Harlan J M 2005 Targeting leukocyte integrins in human diseases *J. Leukoc. Biol.* **77** 129–40

Zaman M H, Trapani L M, Siemeski A, Mackellar D, Gong H Y, Kamm R D, Wells A, Lauffenburger D A and Matsudaira P 2006 Migration of tumor cells in 3D matrices is governed by matrix stiffness along with cell-matrix adhesion and proteolysis *Proc. Natl Acad. Sci. USA* **103** 10889–94

Zhang X, Jiang G, Cai Y, Monkley S J, Critchley D R and Sheetz M P 2008 Talin depletion reveals independence of initial cell spreading from integrin activation and traction *Nat. Cell Biol.* **10** 1062–8

Zigmond S H 1977 Ability of polymorphonuclear leukocytes to orient in gradients of chemotactic factors *J. Cell Biol.* **75** 606–16